GEOPHYSICAL RESEARCH LETTERS, VOL. 23, NO. 8, PAGES 877-880, APRIL 15, 1996

Non-double-couple earthquake mechanisms at The Geysers geothermal area, California.

Alwyn Ross[1] and G. R. Foulger[1]
Dept. Geological Sciences, University of Durham, Durham, U.K.

Bruce R. Julian[2]
Branch of Seismology, U.S. Geological Survey, Menlo Park, California, U.S.A.

Abstract. Inverting *P*- and *S*-wave polarities and *P:SH* amplitude ratios using linear programming methods suggests that about 20% of earthquakes at The Geysers geothermal area have significantly non-double-couple focal mechanisms, with explosive volumetric components as large as 33% of the seismic moment. This conclusion contrasts with those of earlier studies, which interpreted data in terms of double couples. The non-double-couple mechanisms are consistent with combined shear and tensile faulting, possibly caused by industrial water injection. Implosive mechanisms, which might be expected because of rapid steam withdrawal, have not been found. Significant compensated-linear-vector-dipole (CLVD) components in some mechanisms may indicate rapid fluid flow accompanying crack opening.

Introduction

Non-double-couple (non-DC) earthquakes, whose seismic radiation is inconsistent with shear faulting, have recently been found at many volcanic and geothermal areas throughout the world [*Miller et al.*, 1995]. Surprisingly, however, most mechanisms published for earthquakes at the intensely seismically active Geysers geothermal area in northern California are of DC type [*e.g.*, *Oppenheimer*, 1986]. Almost all mechanisms have been derived solely from the polarities of *P*-wave first motions, which have limited information content and resolving power. *O'Connell and Johnson* [1988] obtained a non-DC mechanism for one of three earthquakes studied by inverting waveforms, but attributed this result to error. In this study, we obtain focal mechanisms of higher quality, using *P*- and *S*-wave amplitude data along with polarities, to determine whether non-DC earthquakes do in fact occur at The Geysers.

The Geysers is the most intensively exploited geothermal field in the world. The area experiences about 140 earthquakes of $M_L > 1.2$ per month, and events in recent years have local magnitudes up to 4.9 (UCB). Although the pre-production activity level is poorly known, it is clear that most of the earthquakes are induced by steam removal and water injection [*Stark*, 1990].

[1]Dept. Geological Sciences, University of Durham, South Road, Durham, U.K. DH1 3LE and also at USGS, Menlo Park, CA 94025 (e-mail: alwyn.ross@durham.ac.uk, g.r.foulger@durham.ac.uk).
[2]U.S. Geological Survey, MS 977, 345 Middlefield Road, Menlo Park, CA 94025. (e-mail: julian@andreas.wr.usgs.gov).

Paper number 96GL00590
0094-8534/96/96GL-00590$05.00

Data and Method

In April 1991 we deployed a temporary network of fifteen, three-component PASSCAL digital seismic stations with Mark Products model L22D 2-Hz sensors and REFTEK model 72A-02 data loggers in an array 15 km in diameter at The Geysers (Figure 1). We recorded continuously at a sampling rate of 100 sps and detected about 4000 local earthquakes. The network geometry provided good focal-sphere coverage for events in the central, most active part of the geothermal area. In addition, the UNOCAL Corporation operates 22 seismometers in the area and the U.S. Geological Survey (USGS) 18.

Seismic-wave amplitudes are strongly distorted by geometric spreading of rays, to which *P:S* amplitude ratios are relatively insensitive. We therefore used linear-programming methods [*Julian*, 1986; *Julian and Foulger*, 1995] to invert *P*- and *SH*-wave polarities and *P:SH* amplitude ratios and determine seismic moment tensors. We supplemented polarity and amplitude data recorded on the temporary network with polarity data from USGS stations. Data from the UNOCAL network contributed only to estimating earthquake locations, and not focal mechanisms, because the instrument polarities are unknown.

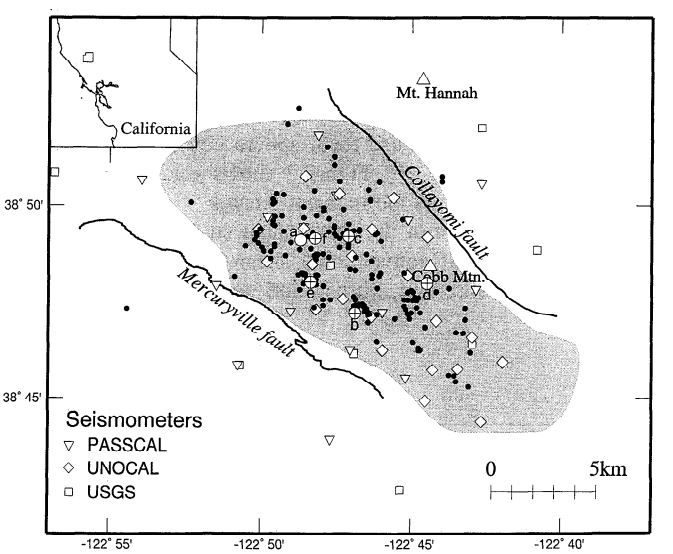

Figure 1. Map of The Geysers geothermal area, California, showing the steam production area (shaded), events used to derive the tomographic velocity structure (black dots) [*Julian et al.*, 1996] and events (a-f) for which focal mechanisms are shown in Figure 3. Seismic stations are also shown.

The seismograms recorded on the PASSCAL instruments were first processed to remove acausal effects of anti-alias filtering in the recorder (J. Fowler, personal communication, 1993) and then low-pass filtered (three-pole Butterworth response, 5 Hz corner frequency) to reduce the effects of wave scattering and attenuation. Rays were numerically traced [*Julian and Gubbins*, 1977] through high-quality velocity models of V_P and V_S [*Julian et al.*, 1996] as part of the process of determining hypocenter locations and mapping rays onto focal spheres. *P*-wave amplitudes were measured on vertical-component seismograms. *SH*-wave amplitudes were measured on transverse-component seismograms obtained by numerically rotating the digital seismograms. Amplitudes were measured from the first onset to the first peak, and only signals with similar rise times were used in ratios. We corrected amplitudes for the effect of the free surface and multiplied amplitudes by the cube of the wave speed at the focus to approximately eliminate systematic differences in *P*- and *S*-wave amplitudes (see *Aki and Richards* [1980], eqn. 4.91).

Wave attenuation affects compressional and shear waves differently, multiplying *P:S* amplitude ratios by

$$\exp\left(-\frac{\omega}{2}\left[\frac{t_p}{Q_p}-\frac{t_s}{Q_s}\right]\right).$$

where ω is angular frequency, Q_p and Q_s are the figures of merit for compressional and shear waves, and t_p and t_s are their travel times. We corrected for attenuation using $Q_p = 60$, a reasonable value for the reservoir [*Zucca et al.*, 1993] and a range of values for Q_s, which has not been measured at The Geysers. We present results for $Q_s = 84$ ($Q_s/Q_p = 1.4$, appropriate for attenuation by scattering from cracks and voids [*Menke et al.*, 1995]). A value as low as $Q_s = 27$ ($Q_s/Q_p = 0.45$, appropriate for attenuation by shear anelasticity), does not change the results enough to affect the conclusions of this paper.

Results

We studied focal mechanisms for 24 of the best-recorded earthquakes in detail. Hypocenter locations (Figures 1 and 2) were determined using up to 39 *P*- and 12 *S*-wave arrival times. The events were distributed throughout the deeper parts of the seismogenic volume because focal sphere coverage was best for those events (Table 1). Figure 3 shows solutions for six events and Table 2 gives the moment tensors.

The results for most of the earthquakes studied are close to DCs and, in terms of conventional shear-faulting interpretations, include strike-slip, thrust and normal orientations.

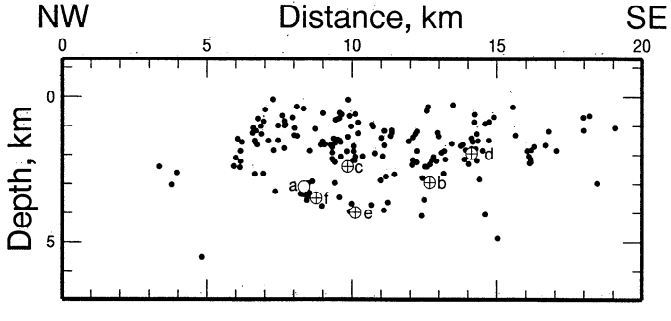

Figure 2. NW-SE cross-section showing hypocenters of the events illustrated in Figure 1. Symbols as in Figure 1.

Table 1. Origins and magnitudes of the earthquakes studied.

event	date, origin time	latitude longitude	depth bsl, km	moment mag M^1
a	91/04/30 01:37:39.22	38.8183 -122.8116	3.10	1.77
b	91/4/14 00:23:50.30	38.7867 -122.7812	2.95	2.75
c	91/4/17 16:41:38.00	38.8199 -122.7850	2.40	2.02
d	91/4/21 09:36:49.29	38.7996 -122.7412	1.94	2.09
e	91/4/26 05:29:27.17	38.8001 -122.8060	3.99	1.88
f	91/4/27 06:29:31.08	38.8190 -122.8035	3.49	1.84

[1] $\log M_0 = 1.5M + 16$ (M_0 in N m)

Figure 3a shows a good example. Focal-mechanism solutions for the five earthquakes shown in Figure 3b-f depart strongly from DCs. These earthquakes all have areas of compression dominating the focal sphere, with one earthquake (event b) exhibiting no dilational arrivals. The explosive components comprise 20-33% of the total moment and indicate volume increases at the sources. Similar solutions are obtained if only *P*-wave polarities are used. Events b and f are particularly good examples.

The orientations of the principal axes of the moment tensors vary considerably, suggesting a locally heterogeneous stress field. In general, the P axes tend to be sub-horizontal and trend NW through NE. The T-axes tend to trend more east-west.

Discussion

In our limited data set about 20% of earthquakes at The Geysers have substantial non-DC components that include volume increases of up to 33%. Figure 4 shows a "source type plot" of the six events shown in Figure 3 [*Hudson et al.*, 1989]. About half of these lie between the DC and +Crack loci on the source type plot (earthquakes e, c and d) and thus may be explained by combined shear and tensile faulting. Earthquakes b and f lie between the +Crack and +CLVD loci and thus depart from the simple shear/tensile-fault model. They might be interpreted as opening cracks that are partially compensated by fluid flowing into the crack [*Julian*, 1983]. Such a process is likely in The Geysers, where earthquakes are induced by major changes in pore fluid pressure caused by the extraction of steam and reinjection of water.

Fluid injection would be expected to increase pore pressure, and thus to encourage crack opening and explosive mechanisms. *Stark* [1990] showed that some microearthquakes at The Geysers cluster around injection wells. The epicenters of events b, c and e are less than 600 m from injection wellheads, which supports the theory that they may be induced by local pressure increases caused by injection.

The removal of large volumes of steam at The Geysers has greatly decreased pore pressure, which might be expected to encourage events with implosive mechanisms. These were not well constrained in this study, though 1-2% of the best-constrained earthquakes of *Oppenheimer* [1986] are dominated by dilational arrivals [*Julian et al.*, 1993]. Implosive

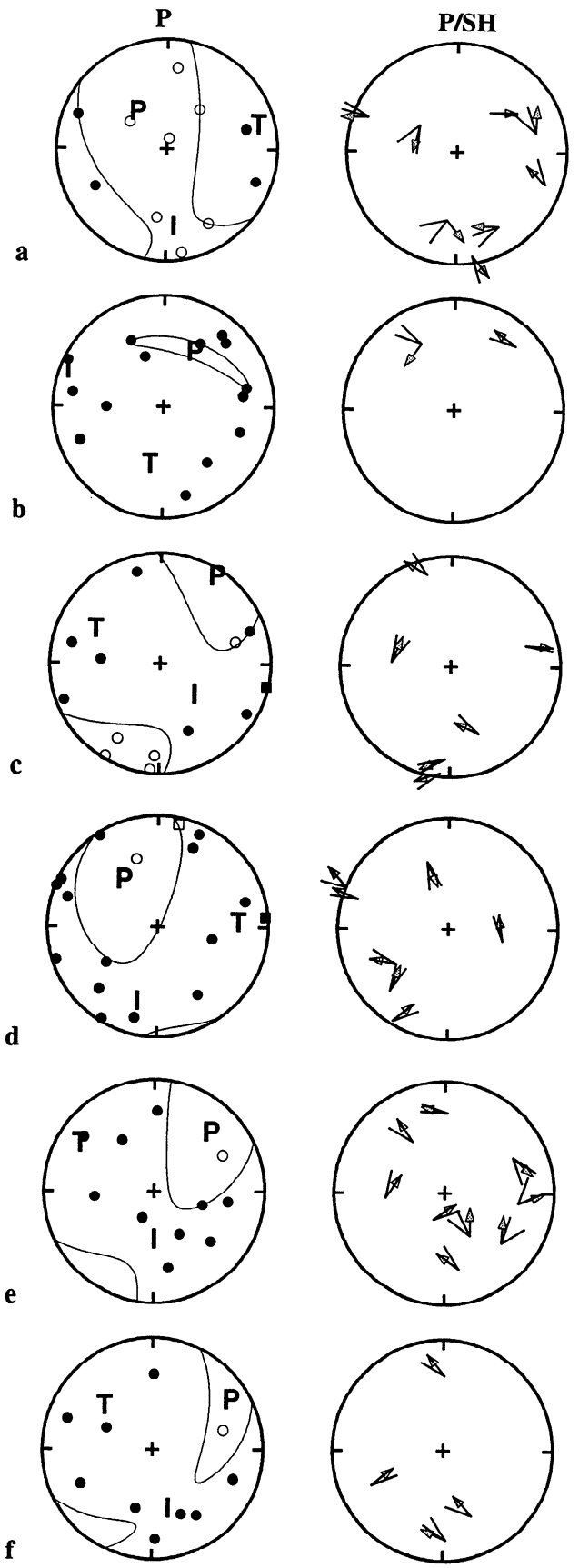

Table 2. Relative moment tensor components for events.

event	Relative moment tensor components					
	M_{xx}[1]	M_{xy}	M_{yy}	M_{xz}	M_{yz}	M_{zz}
a	-5.06	10.45	19.15	6.54	-13.43	-14.96
b	18.34	3.83	1.30	20.55	4.74	22.12
c	-1.17	-15.65	16.74	-5.23	13.03	14.27
d	-1.98	7.08	24.56	9.66	-19.34	-1.05
e	5.64	-19.96	18.36	-1.60	14.06	4.73
f	8.40	-10.88	8.69	-10.48	12.79	14.39

[1] Component coordinate system, x = north, y = east, and z = down.

earthquakes have been reported from the Krafla geothermal area, Iceland, but their first arrivals are less impulsive than those of explosive earthquakes there [*Arnott and Foulger*, 1994]. Earthquakes of this kind may be difficult to observe because cavity collapse may occur relatively slowly and excite seismic radiation inefficiently. Also, earthquakes induced by steam extraction may tend to be smaller and shallower than injection-induced earthquakes and thus poorly constrained by this study.

The observations presented here add to the mounting volume of evidence for non-DC earthquakes in geothermal areas. Future studies of earthquakes in geothermal areas should be designed to detect non-DC focal mechanisms, as this information may be key to understanding the processes of fluid movements in the reservoir. Furthermore, the importance of fluids in the nucleation of earthquakes and in the propagation of failure is becoming increasingly appreciated. A broader search for non-DC components in focal mechanisms thus has the potential to increase our understanding of earthquake processes in general.

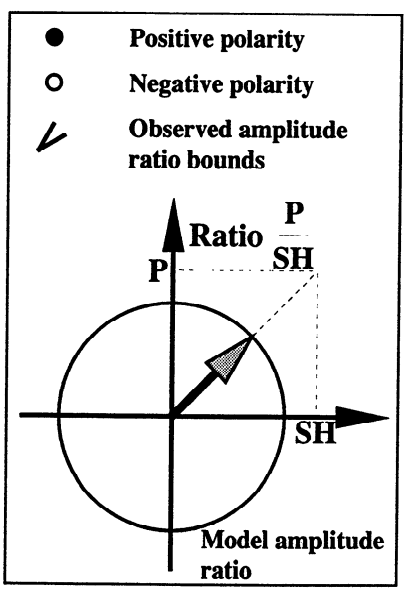

Figure 3. Focal mechanisms of six well-constrained earthquakes at The Geysers. Left: *P*-wave polarities; right: *P:SH*-wave amplitude ratios; open symbols: dilations; filled symbols: compressions; squares: lower-hemisphere observations plotted at their antipodal points. Theoretical amplitude ratios are represented as the directions of small arrows and pairs of lines indicate ranges compatible with the observations (see key). Upper focal hemispheres in equal-area projection.

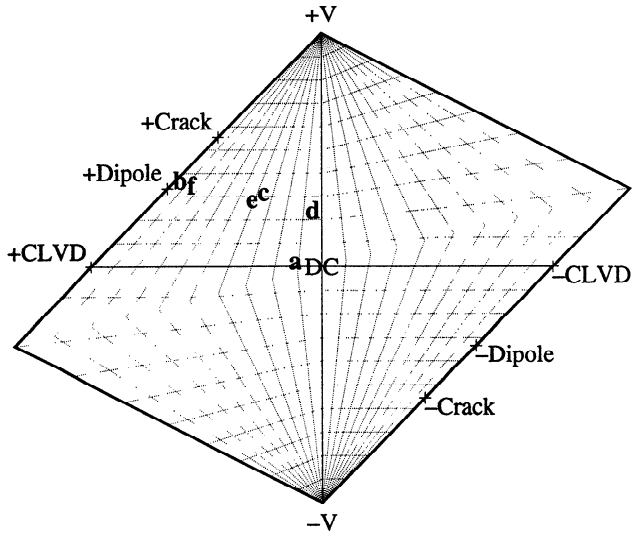

Figure 4. Equal-area "source type plot" [*Hudson et al.*, 1989] showing the earthquake mechanisms studied. The horizontal position shows the ratio of the CLVD component to the non-volumetric (CLVD+DC) component. The vertical position shows the volumetric component. Letters a-f correspond to earthquakes shown in Figures 1-3 and Tables 1 and 2. ±V: Isotropic volume changes; ±Dipole: Linear vector (force) dipoles; ±CLVD: Compensated linear vector dipoles; ±Crack: Opening and closing tensile cracks.

Conclusions

1. Study of a limited set of data suggests that about 20% of the earthquakes at The Geysers have substantial non-DC components.
2. Some earthquakes have explosive volumetric components of up to about 33%. Approximately half of these are consistent with combined shear and tensile faulting. The rest have significant CLVD components that may indicate fluid flow accompanying failure.
3. The non-DC events studied are probably caused by reinjection of water. Steam extraction might be expected to cause implosive earthquakes, but these are not well-constrained, and may be fundamentally more difficult to observe.

Acknowledgments. We thank M. Stark, S. Davis, W. Cumming and the UNOCAL Corporation for assistance and data. A. Miller and S. D. P. Williams assisted with software and helpful discussions. This work was supported by a USGS G. K. Gilbert Fellowship. NERC Grant GR9/134 and a loan of IRIS/PASSCAL equipment. A. R. was supported by a Ph.D scholarship from the Dept. of Education for Northern Ireland. Any use of trade names and trademarks in this publication is for descriptive purposes only, and does not constitute endorsement by the U.S. Government.

References

Aki, K, and P. G. Richards, *Quantitative Seismology,* vol 1, Freeman, New York, pp 557, 1980.

Arnott, S. K., and G. R. Foulger, The Krafla spreading segment, Iceland: 2. The accretionary stress cycle and non-shear earthquake focal mechanisms, *J. Geophys. Res.*, 99, 23827-23842, 1994.

Hudson, J. A., R. G. Pearce, and R. M. Rogers, Source type plot for inversion of the moment tensor, *J. Geophys. Res.*, 94, 765-774, 1989.

Julian, B. R., Evidence for dyke intrusion earthquake mechanisms near Long Valley Caldera, California, *Nature,* 303, 323-325, 1983.

Julian, B. R., Analysing seismic-source mechanisms by linear-programming methods, *Geophys. J. R. astr. Soc.*, 84, 431-443, 1986.

Julian, B. R., and G. R. Foulger, Moment tensors from linear inversion of body-wave amplitude ratios: Powerful constraints on earthquake mechanisms, submitted to *Bull. Seis. Soc. Am.*, 1995.

Julian, B. R., and D. Gubbins, Three-dimensional seismic-ray tracing, *J. Geophys.*, 43, 95-113, 1977.

Julian, B. R., A. D. Miller, and G. R. Foulger, Non-shear focal mechanisms of earthquakes at The Geysers, California, and Hengill, Iceland, geothermal areas, *Trans. Geotherm. Res. Council*, 17, 123-128, 1993.

Julian, B. R., A. Ross, and G. R. Foulger, Three-dimensional seismic image of a geothermal reservoir: The Geysers, California, in press, *Geophys. Res. Lett.*, 1996.

Menke, W., V. Levin and R. Sethi, Seismic attenuation in the crust at the mid-Atlantic plate boundary in south-west Iceland, *Geophys. J. Int.*, 122, 175-182, 1995.

Miller, A. D., G. R. Foulger, and B. J. Julian, Non-Double-Couple earthquakes II. Observations, submitted to *Rev. Geophys.*, 1995.

O'Connell, D. R. H., and L. R. Johnson, Second-order moment tensors of microearthquakes at The Geysers geothermal field, California, *Bull. Seis. Soc. Am.*, 78, 1674-1692, 1988.

Oppenheimer, D. H., Extensional tectonics at The Geysers geothermal area, California, *J. Geophys. Res.* 89, 1191-1207, 1986.

Stark, M. A., Microearthquakes- a tool to track injected water in The Geysers reservoir, *Trans. Geotherm. Res. Coun,* 14, 1697-1704, 1990.

Zucca, J.J., L.J. Hutchings and P.W. Kasameyer, Seismic velocity and attenuation structure of The Geysers geothermal field, CA., *Geothermics*, 23, 111-126, 1993.

(Received October 24, 1995; revised February 5, 1996; accepted February 12, 1996)